MINERALOGICAL MAGAZINE, DECEMBER 1984, VOL. 48, PP. 495–505

Rare-earth element distribution in the metabasic rocks of the Land's End granite aureole, SW England

P. MITROPOULOS

Department of Geology, University of Athens, Panepistimiopolis, Ano Ilisia, Athens 15771, Greece

ABSTRACT. Rock samples from the various metabasic hornfelses of the Land's End granite aureole were analysed for major elements by X-ray fluorescence analysis and for rare-earth elements (*REE*) by instrumental neutron activation analysis (INAA). The *REE* patterns of the unaltered dolerites of the area seem to be analogous to those of the alkali basalts, taking into account a slight mobilization of the light *REE* during low-grade metamorphism.

The *REE* content of the metabasic rocks of the aureole has increased relative to that of the unaltered dolerites due to the introduction of *REE*, along with K, from the granite by the action of hydrothermal solutions. The parallel increase in *REE* with the increase in K is demonstrated.

The metasomatic hornfelses of igneous origin form two groups showing slightly different *REE* patterns and different rates of increase in *REE* content. The *REE* patterns of the two groups show a Eu anomaly increasing with the increase in *REE* content for the first group and decreasing with the increase in *REE* content for the second group, A qualitative model of the distribution of the *REE* in the metabasic aureole rocks is given.

THE great variety of the metamorphic–metasomatic hornfelses which exist in the Land's End granite aureole, as well as the rich mineral veining of the area, have attracted the interest of a great number of geologists since the beginning of the last century. A detailed review of the previous research on the Land's End granite aureole is given in Mitropoulos (1979). The mineralogically, petrologically, and chemically different aureole rock types are regarded as derived by metamorphism, coupled with metasomatism, of basic igneous and sedimentary rocks resulting from the introduction of the granite.

It has been shown (Mitropoulos, 1982) that the metasedimentary hornfelses of the Land's End granite aureole show similar *REE* patterns, highly enriched in light *REE* relative to the heavy *REE*. The *REE* content of the metasedimentary hornfelses of the aureole has increased relative to the *REE* content of the unaltered sediments of the area due to the introduction of *REE* from the granite by the action of hydrothermal solutions. It has also been shown that the *REE* patterns of the metasedimentary hornfelses of the Land's End granite aureole have a completely different shape to the patterns of both the metabasic rocks of the aureole and the granite.

The present work is an attempt to trace possible genetic relationships between the different metabasic hornfelses occurring in the Land's End granite aureole using *REE* geochemistry.

Geological setting

The Land's End peninsula, lying in the western part of Cornwall, is formed of a mass of granite surrounded by a narrow belt of metamorphosed and metasomatized basic igneous and sedimentary country rocks still exposed at various points along the coastline (fig. 1). The Land's End granite is one of the six exposed parts of the Cornish batholith dated at between 270 and 290 Ma (Dodson and Rex, 1971). The sedimentary rocks, assigned to the Mylor series, occurring in the Land's End granite aureole, are of late Middle Devonian to early Late Devonian age. More details on the geology of the granite and the sedimentary rocks of the area are given in Mitropoulos (1979, 1982).

The basic rocks of SW Cornwall consist of doleritic masses intruding irregularly through sedimentary rocks, doleritic sills, and spilitic pillow lavas. All these basic bodies are unquestionably of magmatic origin, having metamorphosed the sedimentary rocks (Flett, 1903). As they also show metamorphic–metasomatic alteration by the granite, they are of pre-granite age. Geochemically, they seem to be representatives of continental alkaline basalts (Floyd, 1972, 1976). Floyd also suggested that these intrusives are the moderately well differentiated basaltic products of a primary magma derived from a subduction zone. This

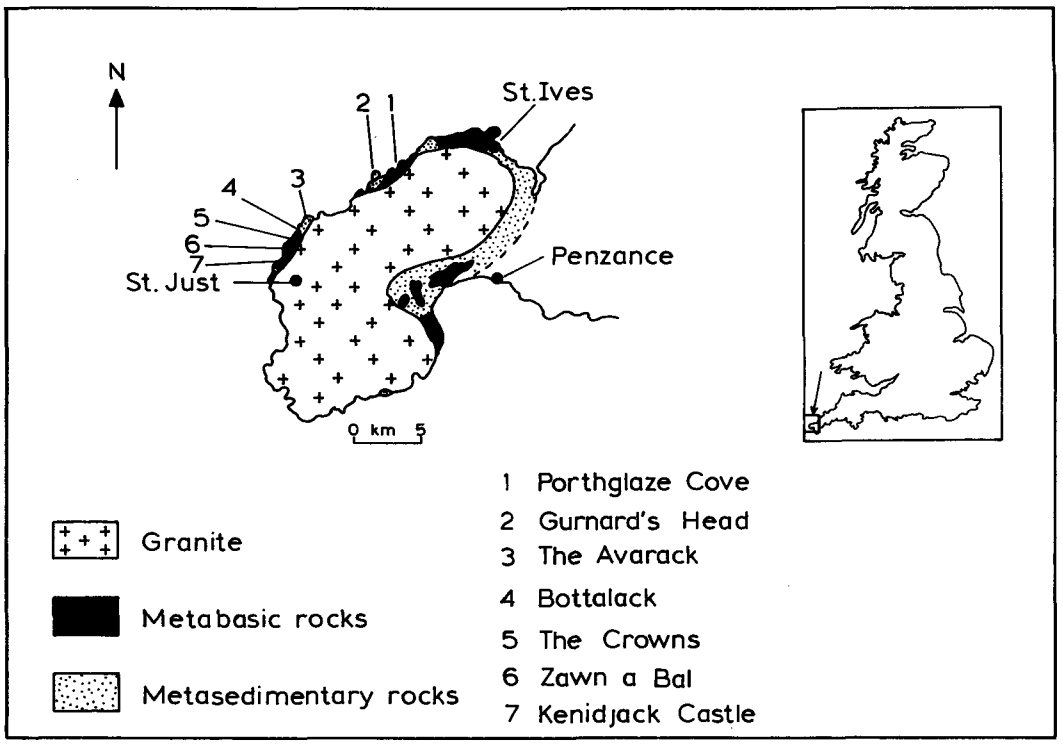

FIG. 1. Geological sketch map of the Land's End area, SW England, showing the sample locations.

subduction zone, active during the Devonian-Carboniferous period, existed between an essentially static European plate of continental crust composition and a north-eastward moving African plate, of oceanic crust composition, which culminated in the Armorican-Variscan orogeny.

The basic intrusive rocks occurring in the Land's End granite aureole have been converted to various types of hornfelses. Khan (1972) applied Q-mode cluster analysis and R-mode factor analysis on the basis of twenty-three major and trace elements to group the metabasic rocks of the aureole. He recognized the following major zones of metasomatic alteration or deposition (fig. 2).

(*a*) Zone of high-grade metamorphic cordierite ± biotite ± Fe-Mg amphibole hornfelses. The rocks show a fine grained compact texture and development of large areas of cordierite which appears to be replacing plagioclase. Sometimes irregular biotite flakes, replacing Fe-Mg amphiboles, and streams of ilmenite granules appear, probably due to late-stage hydrothermal activity.

(*b*) Zone of cummingtonite ± anthophylite ± cordierite ± plagioclase hornfelses, lying around the high-grade cordieritic horizon. In thin section cummingtonite appears as a mass of compact radiating bundles, or large scattered acicular crystals. Actinolite-bearing rocks or veins are associated with the rocks of this zone giving evidence of retrogression and Fe-Mg mobility. In the same group anthophyllite ± spinel ± diaspore hornfelses are included, which may represent the most extreme variant of the cummingtonite ± cordierite-bearing hornfelses.

(*c*) Zone of biotite-hornblende hornfelses. In the low-grade metadolerites of this zone, biotite is present around ilmenite grains, replacing hornblende. The extensive biotitization in this zone is due to the higher mobility of K as a result of the instability of biotite in higher temperature zones and the lack of an orthoclase phase in the high-grade igneous hornfelses. The biotite which is present alongside cordierite in the high grade metadolerites probably formed at a late hydrothermal stage.

(*d*) Zone of hornblende ± plagioclase ± sphene hornfelses. These hornfelses have been produced from the original dolerites, on low-grade metamorphism. Sometimes the hornblende pseudomorphed augite.

There are also in the area some calc-silicate hornfelses containing more than 80–90% of Ca-

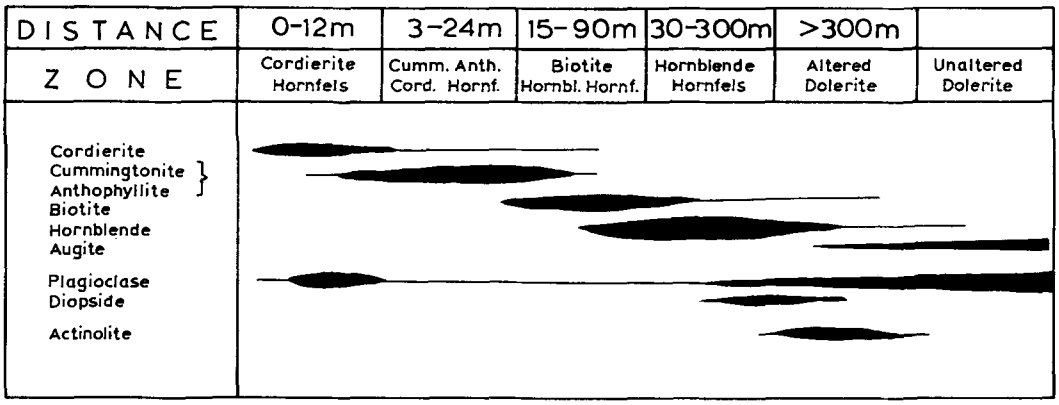

FIG. 2. Mineralogy of the major zones of the metabasic rocks of the aureole, after Khan (1972).

rich minerals, such us diopside, sphene, grossularite, labradorite, clinozoisite, zoisite, epidote, and axinite. These calc-silicate hornfelses show very complicated geochemical characteristics, so their *REE* geochemistry will be examined in a separate paper.

It must be noted that the zonal phenomena observed in the area are substantially after the pattern described by Khan (1972). It is, however, apparent that the widths of the different metasomatic zones developed within the aureole are highly variable and their geometrical boundaries are irregular. This must be due to the fact that the zonal arrangement of the various aureole rock types is not only controlled by their direct distance from the granite contact but also by the complexity of the joint system which is very important in directing the flow of the hydrothermal solutions producing the various metasomatic rock types.

Sampling and analysis of the metabasic rocks

Samples from all the different metasomatic zones of the igneous rocks (dolerites and pillow-lavas) of the aureole, described by Khan (1972), were collected. The collection of these samples was extended to different localities (fig. 1) where the metasomatic aureole rocks occur, in order to show a general pattern of possible variation. Samples were also collected from unmetamorphosed basic rocks outside the aureole, to serve as a basis for comparison.

A thin section was prepared from each sample for microscopic analysis (Table I). The most representative samples from each zone were selected for analysis by instrumental neutron activation analysis for the *REE*, on the basis of the microscopic analysis and of the major-element chemistry.

The samples were analysed for major elements and for La and Ce by X-ray fluorescence (XRF) analysis and for the rest of the *REE* by instrumental neutron activation analysis (INAA; Table II). For the XRF analysis a Philips PW1450 automatic spectrometer with a PW1466 sixty position sample changer was used. The method used was essentially that described by Leake *et al.* (1969). For the INAA, a procedure analogous to that described by Gordon *et al.* (1968), Hertogen and Gijbels (1971), Plant *et al.* (1976), and Jacobs *et al.* (1977) was used. The samples were irradiated in the Herald reactor at the Atomic Weapons Research Establishment, Aldermaston, at a thermal neutron flux of 2.5×10^{12}–$4{\cdot}0 \times 10^{12}$ n cm^{-2} s^{-1} for *c.* 18 h. The total integrated dose received by the samples was 1.0×10^{16} n cm^{-2}. The γ-ray spectra were measured by the use of an Ortec low-energy lithium-drifted germanium spectrometer, mounted horizontally. The spectrometer was connected via an Ortec cryogenic pre-amplifier to an Ortec amplifier and finally to a Northern Scientific NS700 multichannel analyser of 2048 channels. Details on the instrumental conditions, the calibration, and the precision and accuracy of both the methods are given in Mitropoulos (1979, 1982).

REE patterns

In Table II the *REE* values are given for the metabasic rock samples analysed by INAA, along with the *REE* values for the unaltered sedimentary rock sample F99 and the granite rock sample A29. For the presentation of the *REE* patterns normalization of the *REE* abundances in the analysed samples to the abundances in chondrites given by Frey *et al.* (1968) was used.

As has already been noted the analysed rock

TABLE I. Localities and mineralogical description of the analysed rock samples

Sample No	Description	Locality	Mineralogy
	BASIC INTRUSIONS		
A25	least altered dolerite	St. Ives	hornblende-pyroxene (remains) -plagioclase-ilmenite(→ sphene)
F34	least altered dolerite	St. Ives	hornblende-pyroxene (remains) -plagioclase-ilmenite(→ sphene)
A9	least altered biotitised dolerite	Porthglaze Cove	biotitised hornblende-pyroxene (remains)-plagioclase-ilmenite
B32	hornblende hornfels	Gurnard's Head	hornblende-plagioclase -ilmenite(→ sphene)
A4	hornblende hornfels	Gurnard's Head	hornblende (slightly biotitised) -plagioclase-ilmenite(→ sphene)
B34	hornblende hornfels	Gurnard's Head (east coast)	hornblende (biotitised) -plagioclase-ilmenite(→ sphene)
B33	hornblende hornfels	Gurnard's Head (east coast)	hornblende (biotitised) -plagioclase-ilmenite(→ sphene)
B29B	hornblende-biotite hornfels	Gurnard's Head (west coast)	biotite-hornblende -plagioclase-ilmenite(→ sphene)
B24	hornblende-biotite hornfels	Gurnard's Head	biotite-hornblende -plagioclase-ilmenite
A7	hornblende-biotite hornfels	Gurnard's Head	biotite-hornblende -plagioclase-ilmenite
B43	cummingtonite-cordierite hornfels	Zawn a Bal	cummingtonite-cordierite-green spinel-ilmenite
B60	cummingtonite-cordierite hornfels	Kenidjack Castle	cummingtonite-cordierite-(hornblende)-ilmenite
B5	cummingtonite-cordierite-biotite hornfels	The Crown	cummingtonite-cordierite -biotite(-feldspar)-ilmenite
B46	cummingtonite-cordierite-biotite hornfels	Zawn a Bal	cummingtonite-cordierite -biotite-feldspar
B56	cummingtonite-cordierite hornfels	Kenidjack Castle	cummingtonite(slightly biotitised) -cordierite(→ pinite)-Fe-Ti oxides
B8	cummingtonite-biotite hornfels	The Crown	cummingtonite-biotite-diaspore -green spinel- Fe-Ti oxides
B57	cummingtonite-cordierite-biotite hornfels	Kenidjack Castle	cummingtonite-cordierite -biotite-ilmenite(→ sphene)
B55	cummingtonite-cordierite-biotite hornfels	Wheal Edward Zawn	cummingtonite-anthophyllite cordierite(→ pinite)-biotite - Fe-Ti oxides
B59	anthophyllite hornfels	Kenidjack Castle	anthophyllite-diaspore-green spinel-corundum
B41	cordierite-biotite hornfels	Zawn a Bal	cordierite(→ pinite)-biotite- Fe-Ti oxides-small quartz veinlets
B47	actinolite hornfels	Zawn a Bal	actinolite- green spinel -tourmaline- Fe-Ti oxides
A24	actinolite hornfels	The Crown	actinolite-plagioclase - Fe-Ti oxides
	PILLOW LAVAS		
B30	hornblende hornfels	Gurnard's Head (east coast)	hornblende-plagioclase ilmenite(→ sphene)
B29G	hornblende hornfels	Gurnard's Head (west coast)	hornblende(slightly biotitised) -plagioclase-ilmenite(→ sphene)
B28	cordierite-biotite hornfels	Gurnard's Head (west coast)	cordierite-biotite - Fe-Ti oxides
B39	cordierite-biotite hornfels	The Avarack	cordierite(→ pinite)-biotite - Fe-Ti oxides
B51, B52, B54	cummingtonite-cordierite-biotite-anthophyllite hornfels	Wheal Edward Zawn	cordierite(→ pinite)-biotite -cummingtonite-anthophyllite - Fe-Ti oxides

TABLE II. Major element and REE abundances in the analysed rock samples

Sample No	A25	F34	A9	B32	A4	B34	B33	B29B	B24	A7	B43	B60	B5	B46
(wt.%):														
SiO_2	45.10	45.45	47.25	49.21	44.40	48.93	48.84	48.22	50.77	48.26	43.02	45.88	44.76	40.09
TiO_2	1.56	1.53	2.45	2.01	2.65	2.15	2.01	1.77	2.10	2.22	2.04	3.36	2.82	3.13
Al_2O_3	15.68	13.55	9.87	12.62	14.44	12.99	12.74	15.21	12.67	13.40	10.82	14.73	13.27	16.44
$Fe_2O_3^t$	12.70	12.56	16.44	10.21	13.41	12.61	12.56	10.48	12.78	12.32	12.74	10.56	16.53	12.66
MnO	0.44	n.a.	0.31	0.23	0.31	0.17	0.16	0.14	0.17	0.15	0.24	0.24	0.18	0.10
MgO	9.38	9.00	5.07	8.40	7.04	7.24	7.37	10.35	7.52	8.10	15.47	8.12	12.03	13.63
CaO	6.26	10.37	11.27	13.08	10.43	7.88	8.27	3.85	7.94	7.21	11.79	14.65	2.91	1.38
Na_2O	3.58	2.78	1.63	0.30	2.20	3.03	1.25	2.86	3.66	2.62	1.03	0.88	0.86	0.98
K_2O	0.42	0.31	1.79	0.60	1.54	2.05	2.13	4.32	2.54	2.79	0.80	0.65	2.82	8.61
P_2O_5	0.13	0.12	0.47	0.20	0.23	0.23	0.23	0.13	0.19	0.25	0.15	0.88	0.09	0.27
(ppm):														
La	12.8	11.9	29.6	15.9	21.5	29.2	28.1	20.7	25.9	40.8	18.3	29.6	37.6	38.4
Ce	22.3	23.1	50.1	24.5	37.5	41.6	41.4	33.9	41.7	53.2	39.5	55.6	55.4	57.3
Nd	13.0	13.1	35.0	18.3	18.7	20.5	22.9	16.9	24.4	27.0	24.0	35.7	28.9	39.4
Sm	3.57	3.62	8.88	5.98	6.18	6.39	6.80	4.42	6.47	6.82	5.83	7.83	6.31	9.79
Eu	0.75	0.72	1.36	1.61	1.77	1.56	1.98	1.17	0.84	0.80	1.91	2.77	1.56	2.02
Gd	n.d.	n.d.	9.71	n.d.	6.60	n.d.	7.47	3.36	4.60	7.34	5.51	5.60	5.82	3.10
Tb	0.62	0.68	1.81	0.84	1.06	1.13	1.16	0.67	1.17	1.30	1.07	0.89	0.98	1.56
Tm	0.40	0.42	1.06	0.37	0.34	0.50	0.48	0.44	0.66	0.67	0.61	0.30	0.53	0.46
Yb	2.95	2.90	7.46	2.65	3.49	3.62	3.56	3.20	4.94	5.30	3.53	2.19	3.75	1.35
Lu	0.35	0.37	0.87	0.20	0.43	0.42	0.55	0.33	0.57	0.55	0.66	1.43	0.32	0.82

n.a.= not analysed, n.d.= not detected

B56	B8	B57	B55	B59	B41	B47	A24	B30	B29G	B28	B39	B51	B52	B54
47.16	43.10	43.51	48.20	36.73	48.69	46.06	49.14	48.78	51.64	45.91	47.85	41.07	47.68	51.02
3.00	1.68	4.02	5.82	2.17	2.85	2.10	1.65	1.80	1.50	1.65	2.77	5.05	4.58	5.72
13.11	9.13	14.94	16.64	13.61	14.98	10.33	9.57	14.02	13.69	16.11	18.86	14.61	13.72	19.17
16.18	14.24	14.36	12.90	23.15	14.19	14.48	13.34	10.20	10.03	9.77	11.24	18.26	16.86	9.28
0.19	0.25	0.37	0.03	0.21	0.06	0.25	0.24	0.25	0.27	0.12	0.20	0.13	0.17	0.03
11.95	15.69	8.93	5.56	17.17	7.33	15.84	11.49	7.56	7.82	14.53	4.38	9.31	7.56	3.70
3.05	12.96	8.63	1.76	0.62	1.83	9.06	11.96	13.23	9.52	1.99	4.35	3.61	2.23	1.98
1.35	1.04	0.73	4.84	0.27	1.53	0.63	0.67	1.86	2.88	2.14	3.82	1.37	2.24	6.76
0.92	0.29	1.89	1.82	1.58	4.67	0.28	0.52	0.57	0.80	5.40	3.53	2.44	1.04	1.66
0.13	0.28	0.79	1.07	0.29	0.22	0.11	0.15	0.18	0.14	0.13	0.27	0.96	0.81	1.11
36.8	20.6	31.5	48.1	108.0	39.4	18.4	16.1	15.5	21.1	16.2	23.8	36.5	41.3	41.0
51.7	40.1	45.6	74.7	171.0	56.1	34.1	20.8	25.8	37.6	30.7	31.6	54.7	58.6	68.4
23.8	27.6	28.2	39.8	95.0	28.8	19.7	14.3	15.0	19.6	24.3	21.6	33.7	31.9	39.2
5.33	6.97	7.16	9.33	16.58	6.98	4.69	4.03	4.65	5.71	5.54	5.94	8.21	7.50	9.85
1.05	2.46	2.34	3.46	1.80	2.07	1.49	1.48	1.32	1.56	0.92	1.58	3.23	2.50	3.47
3.57	7.76	3.98	8.15	15.94	4.11	n.d.	3.48	3.11	5.98	5.14	5.60	4.90	7.96	10.06
0.77	1.11	0.95	1.40	2.46	1.00	0.83	0.97	0.80	0.98	0.79	0.88	0.98	1.05	1.44
0.72	1.06	1.17	1.22	1.25	0.40	0.64	0.88	0.52	0.87	0.45	0.52	0.93	0.95	1.34
2.95	n.d.	n.d.	3.46	7.81	3.03	1.75	2.00	2.96	4.77	4.66	4.69	n.d.	1.38	4.76
0.28	0.64	1.59	0.83	1.06	0.88	0.29	0.68	0.55	0.85	0.70	0.70	n.d.	0.90	1.52

samples of igneous origin are classified according to the various metasomatic zones proposed by Kahn (1972) on the basis of their mineralogy and major-element chemistry. According to that classification the *REE* patterns of the analysed rock samples were grouped as follows:

Least-altered dolerites. The main mineralogical characteristic of these rocks is that remains of pyroxene crystals still exist, showing their lower grade of metamorphism. The rock samples A25, F34, and A9 from this zone were analysed by INAA for the *REE* (Table II). The first two, A25 and F34, show the same mineralogy (Table I) and major-element chemistry (Table II). In the third sample, A9, the hornblende appears to be biotitized although remains of pyroxene crystals still exist. Comparing the chemical composition of this sample with that of A25 it can be seen that it is considerably enriched in K, which is considered to be added during biotitization, due to the action of the K-rich solutions under low-temperature conditions (Kahn, 1972).

The *REE* patterns of the three rock samples (fig. 3) seem to be similar, but although the absolute *REE* contents of A25 and F34 (Table II). are about the same, A9 shows an enrichment by a factor of about 2.5, for all the *REE* (heavy and light) relative to the *REE* content of the first two samples. This enrichment means that the K-rich solutions were also rich in *REE*. The biotite structure is characterised by the presence of the large interlayer ionic sites X, which are mainly occupied by the large K ion (ionic radius = 1.33 Å), in twelvefold coordination. Ca (ionic radius = 1.25 Å) substitutes for K in these interlayer sites because the other sites

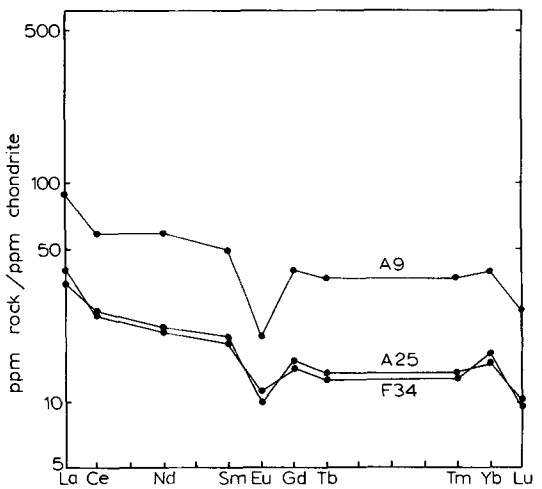

FIG. 3. Chondrite-normalized *REE* patterns of the samples from the zone of the less-altered dolerites.

in the biotite structure are too small to accept it. Ba, Rb, Cs, and Na follow Ca to this substitution (Deer *et al.*, 1962). Because of this it seems probable that the lighter *REE* (large ionic size) can enter the biotite structure as comfortably as the heavier *REE* (smaller ionic size), resulting in a relatively flat *REE* pattern for the biotite (Herrmann, 1970; Hanson, 1978). It seems that, for this reason, the biotitized sample A9 shows this parallel enrichment in all the *REE*.

All the three *REE* patterns (fig. 3) show a negative Eu anomaly which apparently increases with the increase in *REE* content (Eu/Eu*: A25 = 0.62, F34 = 0.60, A9 = 0.45). The probable significance of the Eu anomaly is discussed later in this section. It can be also seen from these *REE* patterns that there is an enrichment in light *REE* relative to the heavy *REE*. In general, alkali basalts show enrichment in light *REE* (Gast, 1968; Sun and Hanson, 1975; Kay and Hubbard, 1978). Floyd (1976), using major-element data, suggested that the dolerites of the area are representatives of continental alkali basalts. In the present work, the sample A25 is considered as representing the most unaltered doleritic material from the analysed rock samples. Comparing the *REE* pattern of this sample with the *REE* patterns of alkali basalts from the literature it appears that the light *REE* enrichment in the sample A25 is lower than in the alkali basalts. In order to confirm Floyd's views about the origin of the dolerites we have to accept that, during the low-grade contact metamorphism, there has been mobilization of the light *REE*, in a way analogous with that found by Wood *et al.* (1976) during zeolite-facies metamorphism of the Tertiary basalts of eastern Iceland. The above comparison of course, is possible only under the assumption that no material, other than H_2O, was introduced into the rock sample A25 from outside.

Hornblende hornfelses. In the rocks belonging to this metasomatic zone, all the initial pyroxene has been converted into hornblende due to the contact metamorphism. The rock samples B32, A4, B34, and B33 from this zone were analysed for the *REE* (Table II). Sample B32 does not show any biotitization but progressive biotitization of the hornblende appears in the samples A4, B34, and B33 (Table I). Comparing the major-element chemistry of the rock samples A4, B34, B33 with that of B32, it can be seen that there is an enrichment in K in a way analogous to that shown in the biotitized rock samples from the zone of the least-altered dolerites, followed by a depletion in Ca.

In fig. 4 the characteristic *REE* patterns of the rock samples of this zone are shown. The patterns of all the four rock samples have a similar shape and they show the same characteristics as the *REE*

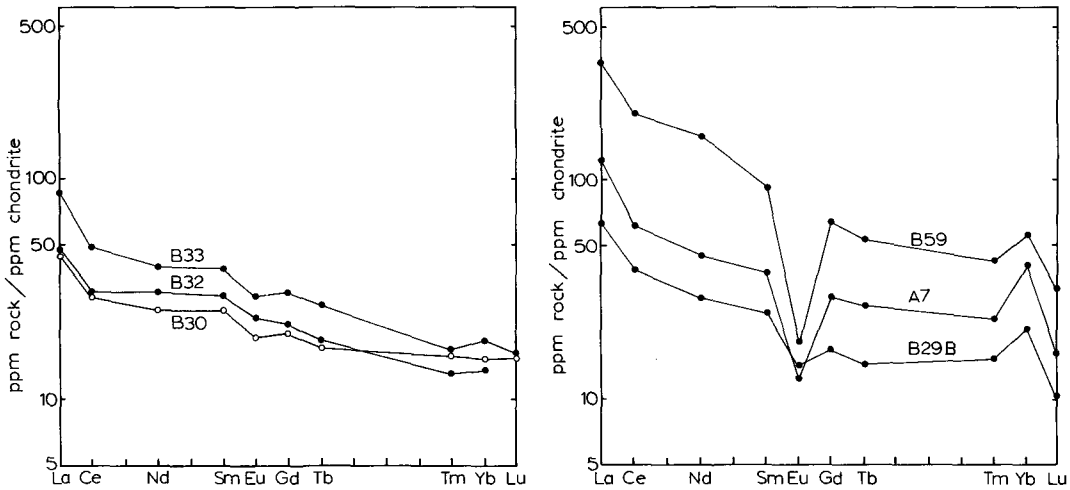

FIGS. 4 and 5. Characteristic chondrite-normalized *REE* patterns. FIG. 4 (*left*). Hornblende hornfelses (open circles: pillow-lava-bearing hornfels). FIG. 5 (*right*). Hornblende-biotite hornfelses (samples B29B and A7) and of anthophyllite hornfelses (sample B59).

patterns of the rock samples from the zone of the least-altered dolerites (fig. 3). These characteristics are:

(*a*) The absolute *REE* content doubles from the non-biotitized sample (B32) to the most biotitized sample (B33).

(*b*) They show a negative Eu anomaly which seems to be increasing with the increase in *REE* content.

(*c*) They show an enrichment in light *REE*.

Samples from the pillow-lava-bearing rocks, which occur in many places in the aureole, were also analysed for the *REE*. The patterns of the analysed samples from this zone (Table II) also show the above described characteristics (fig. 4).

Hornblende-biotite hornfelses. The extensive biotitization of the hornblende is the main mineralogical characteristic of the rock samples of this zone. Three rock samples B29B, B24, and A7 were analysed for the *REE* (Table II). They show, to a higher degree, the same progressive enrichment in K and *REE* as found in the biotitized rock samples from the first two metasomatic zones. The *REE* patterns of these three samples are approximately parallel. The *REE* patterns of the analysed rock samples from this metasomatic zone shown in fig. 5 appear to have the same characteristics as those of the rock samples from the hornblende hornfelses. It seems that in fact there is a continuity between these two metasomatic zones.

Cummingtonite-cordierite-anthophyllite-biotite hornfelses. These rocks have suffered a high degree of metasomatic alteration resulting in a strong depletion in Si and Ca and a major enrichment in Fe and Mg. The latter elements are prominent in minerals such as cummingtonite, anthophyllite, and cordierite. The K content of the rock samples from this zone shows a considerable variation analogous to that found for the rock samples from the previously examined zones. Eight rock samples from this zone, B55, B56, B57, B8, B43, B5, B46, and B60 were analysed for the *REE* (Table II). The patterns of the first five samples are approximately parallel (fig. 6) but show differences compared with the patterns of the rock samples from the previous zones. The main differences are:

(*a*) The enrichment in light *REE* is lower, giving the pattern a slightly different shape. This is probably due to the formation of the Fe-Mg-rich amphiboles in the rocks of this zone. The amphibole structure is characterized by the presence of the *A* 'vacant' structural site which approximately corresponds to the interlayer *X* site of the micas and can accommodate a large cation in ten to twelvefold co-ordination; however, because of the staggering of adjacent double chains of SiO_4 tetrahedra, the effective size of the site is less than in micas (Ernst, 1968). Thus, the heavier *REE*, with the smaller ionic size, can probably enter more easily into the structure of the amphiboles than the light *REE*.

(*b*) They show a negative Eu anomaly for the rock samples with the lower *REE* content. This anomaly becomes smaller and smaller with increasing *REE* content, eventually becoming positive.

The *REE* patterns of the rock samples B5, B46, and B60 from this zone show a degree of similarity

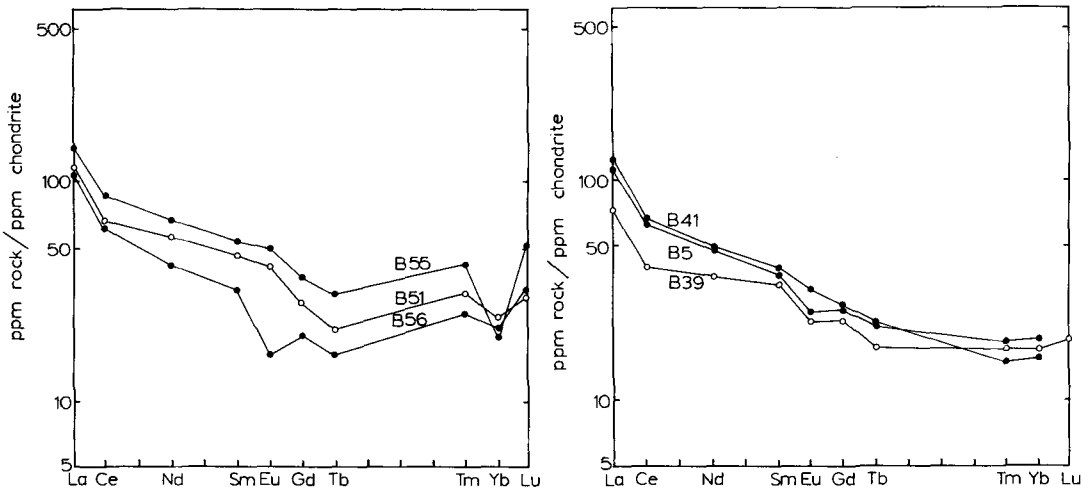

FIGS. 6 and 7. Characteristic chondrite-normalized *REE* patterns. FIG. 6 (*left*). Cummingtonite-cordierite-anthophyllite-biotite hornfelses (open circles: pillow-lava-bearing hornfels). FIG. 7 (*right*). Cordierite-biotite hornfelses (samples B41 and B39) in comparison with the chondrite-normalized *REE* of the sample B5 from the cummingtonite-cordierite-anthophyllite-biotite hornfelses (open circles: pillow-lava-bearing hornfels).

with the *REE* pattern of sample B41 from the zone of cordierite-biotite hornfelses (fig. 7). It seems probable that these three samples represent the transitional zone between the two distinct hornfelsic types.

The rock samples B51, B52, and B54 from the pillow-lava-bearing rocks, having the same mineralogy of this zone, were also analysed for the *REE*. Their patterns are similar, showing the same characteristics (fig. 6) as the patterns of the rock samples described above.

The rock sample B59, consisting mainly of anthophyllite (Table I), was analysed for the *REE* (Table II), as representative of the anthophyllite hornfelses. The *REE* content of this sample is very high, about eight times the content of sample A25 (Table II) and although highly enriched in Fe and Mg, its *REE* pattern (fig. 5) is analogous with the *REE* patterns of the rock samples from the hornblende-biotite metasomatic zone (fig. 5). It shows light *REE* enrichment and a large negative Eu anomaly.

The rock samples A24 and B47 from the actinolite-bearing hornfelses were also analysed for the *REE* (Table II). Their contents are similar to those of the non-biotitized hornblende hornfelses (Table II), but their patterns do not show any Eu anomaly. They show a slight enrichment in light *REE* and in general their patterns show a similarity to the patterns of the rock samples from the cummingtonite - cordierite - anthophyllite - biotite hornfelses.

Cordierite-biotite hornfelses. The higher degree of biotitization occurring in the rock samples of this zone and the incoming of cordierite led to the increase in Si, Al, K, and the decrease in Ca relative to the least-altered dolerites. The *REE* pattern of the sample B41 (fig. 7) from this zone shows enrichment in light *REE*, but does not show any Eu anomaly. The absolute *REE* content of this sample is more than twice the content of the least-altered dolerites.

The *REE* patterns of the analysed rock samples B28 and B39 from the pillow-lava-bearing cordierite-biotite hornfelses (fig. 7) show differences compared with the *REE* patterns of the cordierite-biotite hornfelses from the intrusive basic rocks, such as the presence of a negative Eu anomaly and the lower *LREE*: *HREE* ratio. Khan (1972) noted that there are two types (Botallack type and Gurnard's Head type) of cordierite-biotite-bearing hornfelses in respect of their mineralogical and chemical composition. It seems probable that the two *REE* distributions found for the rocks of this zone correspond to the above two types of cordierite-biotite-bearing hornfelses.

Discussion and conclusions

The majority of the analysed rock samples from the basic igneous rocks of the Land's End granite aureole can be grouped into two major groups according to the common characteristics shown by their chondrite normalized *REE* patterns. The samples of intrusive and pillow-lava-bearing rocks from certain zones, notably the least-

altered dolerites, the hornblende hornfelses, the hornblende-biotite hornfelses, together with the rock samples B28 and B39 from the biotite-cordierite hornfelses and the anthophyllite hornfelses, make up the first group (group I). Group II consists of samples of the intrusive and pillow-lava-bearing rocks from the cummingtonite-cordierite-anthophyllite-biotite hornfelses (excluding the samples B5, B60, B46), and the actinolite hornfelses.

The *REE* patterns of the rocks of group I show an enrichment in light *REE*, and a negative Eu anomaly increasing with the increase in the *REE* content.

The *REE* patterns of the rocks of group II also show an enrichment in light *REE* although the *LREE*:*HREE* ratio seems to be lower than that of group I. The negative Eu anomaly, found in some of the rocks of this group, seems to decrease with increasing *REE* content, becoming positive for rocks with higher *REE* content.

Besides these distinctive characteristics the *REE* patterns of these two groups of the aureole rocks show a number of common characteristics. There is a parallel enrichment in all the *REE* (excluding of course Eu because of its anomalous behaviour). This enrichment was suggested to be related to the K and hence to the Rb and Ba enrichment (Mitropoulos, 1979). In the diagrams of fig. 8 this relationship is demonstrated. The chondrite-normalized values of Nd and Sm, two of the *REE* with normalized values of about the same level of magnitude, are plotted against the K_2O content for each one of the two groups of rocks. For group I, K_2O shows a high positive correlation with both the elements Nd and Sm for a wide range of compositions, with correlation coefficients of 0.90 for Sm and 0.88 for Nd. If the values for sample A9 are excluded, the correlation coefficients rise to 0.98 and 0.95 respectively. For the second group the positive correlation between K_2O and both Nd and Sm is slightly lower (correlation coefficients are 0.81 for Sm and 0.79 for Nd), because of the more widely spread values that these two elements show. This may be due to the differences in relative proportions of constituent minerals coupled with textural inhomogeneity in the rocks of this group.

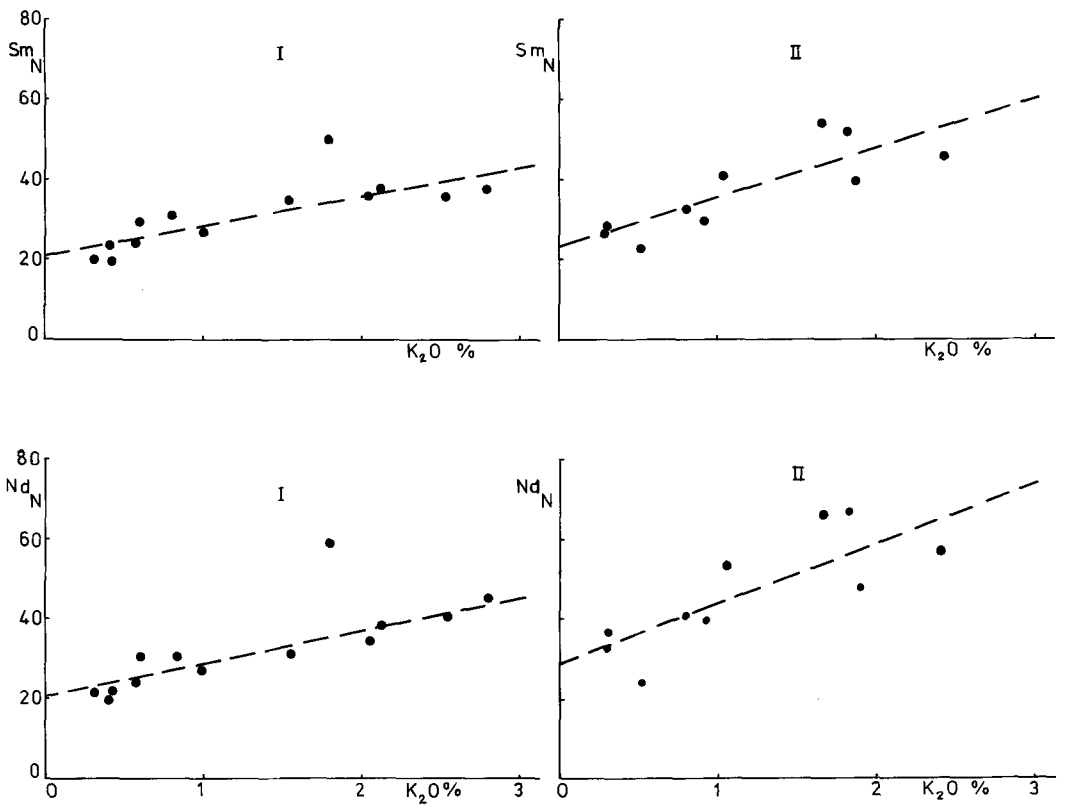

FIG. 8. Nd_N and Sm_N *vs.* K_2O plots for the metabasic rocks of the Land's End granite aureole. Groups I and II defined in the text.

Two more points must be noted from fig. 8. First, that in both the groups there are samples with low *REE* content. The lower *REE* content found in the samples of group I is at about the same level as that found in the samples of group II. This can be taken as an indication that the *REE* have not been removed to any large extent from the Fe-Mg-rich hornfelses (group II) during the course of their formation. Only a small amount of the light *REE* can have been removed from these hornfelses to produce the lower *LREE*:*HREE* ratio. This is related to the higher mobility of the light *REE* under metamorphic conditions (Wood *et al.*, 1976) and to their large ionic size which prevents them from easily entering the structure of the amphiboles formed.

The second point is the higher rate of enrichment for both Sm and Nd in the rock samples of group II as compared with group I. The slopes of the best fitting lines drawn in the four plots are: 7 for Sm and 8 for Nd for the rocks of group I, and 13 and 14 for Sm and Nd respectively for the rocks of group II. This probably means that more *REE* cations were available in the hydrothermal solutions in the areas closer to the granite contact in which the rocks of group II are now found. This is also shown by the fact that between the samples B51 and B54 the sample more enriched in *REE* is B54 (Table II) as its apparent distance from the granite contact is less.

The *REE* patterns of the rocks of the two groups show Eu anomalies which are either positive or negative. The samples A9 of group I and B60 of group II show similar *REE* content (Table II), which means that the same amount of *REE* was added by the hydrothermal solutions in the two samples. However, they show Eu anomalies of different sign (i.e. negative for A9 and positive for B60). It can consequently be suggested that the Eu^{3+} content of the hydrothermal solutions was not stable during their movement to the outer parts of the aureole but depended on the change of the redox conditions, as the Eu^{3+} increases relative to Eu^{2+} under oxidizing conditions. The increasing negative Eu anomaly with the increase in *REE* content in the rocks of group I can be taken as an indication of a decreasing oxygen fugacity for the hydrothermal solutions. In group II, because the negative Eu anomaly decreases with increasing total *REE* content finally reversing to became a positive anomaly, it would seem that the higher *REE* contents are associated with higher oxygen fugacity of the hydrothermal solutions. This is supported by the development of sphene from ilmenite, a reaction common in these rocks (Table I), which takes place under oxidizing conditions (Czamanske and Mihalik, 1972).

Sample B59 from the anthophyllite hornfelses shows a high *REE* content (Table II), but although it shows major element characteristics similar to those of the rocks of group II (i.e. high Fe-Mg enrichment, depletion in Si and Ca) and its apparent distance from the granite contact is small, its *REE* pattern shows the same characteristics as those of the rocks of group I. In order to explain the phenomenon, more analytical data on the *REE* content of separated minerals are needed. However, it can be suggested that the hydrothermal solutions reaching the B59 locality had passed through adjacent sedimentary rocks (fig. 1), which in general show a high *REE* content (Mitropoulos, 1982). Because of this, the *REE* content of the hydrothermal solutions was higher, producing the high *REE* enrichment observed. Analogous suggestion may account for the unusual appearance of the *REE* patterns of the samples B5, B60, and B46 from the cummingtonite-cordierite-biotite-anthophyllite hornfelses.

It must be emphasized at this point that the *REE* distribution in the rocks of the aureole does not only depend on their apparent distance from the granite contact. The flow of the solutions through the rocks is determined by their permeability. In this context, the complex joint system is very

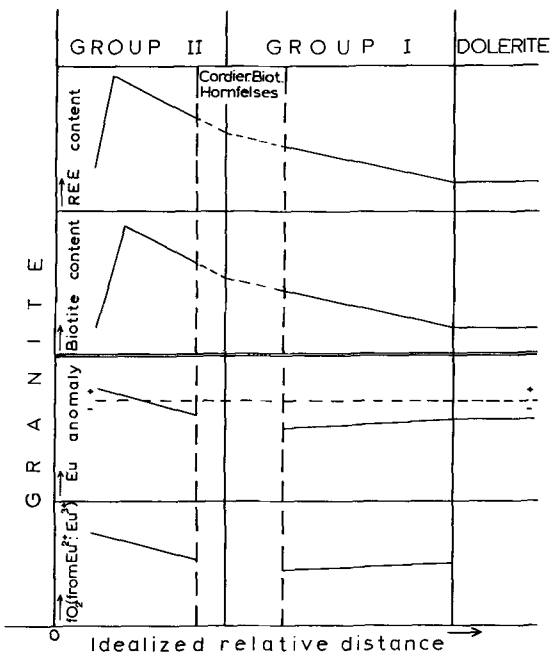

FIG. 9. Qualitative model of the distribution of the *REE* in the metabasic rocks of the Land's End granite aureole. Groups I and II defined in the text.

important in directing the flow and hence in determining the location of the maximum metasomatic effects. It may be useful to introduce the idealized zonal arrangement concept of Curtis and Brown (1969, 1971). Certainly the metasomatic effects in the Land's End rocks are subject to rapid and often rather capricious lateral variation.

Summarizing all the characteristics of the metabasic rocks of the aureole discussed above, a qualitative model of the distribution of the *REE* in these rocks can be given (fig. 9).

Acknowledgements. I am grateful to Mr E. D. Lacy along with Dr G. L. Hendry for their advice and encouragement throughout my research, carried out at Birmingham University, and to the State Scholarships Foundation of Greece for the financial support. The SRC grant for use of irraditation facilities is also acknowledged.

REFERENCES

Curtis, C. D., and Brown, P. E. (1969) *Contrib. Mineral. Petrol.* **24,** 275–92.
———(1971) Ibid. **31,** 87–93.
Czamanske, G. K., and Mihalik, P. (1972) *J. Petrol.* **13,** 493–509.
Deer, W. A., Howie, R. A., and Zussman, J. (1962) *Rock Forming Minerals*, **3.** Longmans, London.
Dodson, M. H., and Rex, D. C. (1971) *Q.J. Geol. Soc. London*, **126,** 465–99.
Ernst, W. G. (1968) *Amphiboles.* Springer-Verlag, Berlin.
Flett, J. S. (1903) *Petrography of West Cornwall.* G.B. Geol. Surv. Sum. Prog. pp. 150–62.
Floyd, P. A. (1972) *Proc. Geol. Assoc.* **83,** 385–404.
——(1976) J. Petrol. **17,** 522–45.
Frey, F. A., Haskin, M. A., Poetz, J. A., and Haskin, L. A. (1968) *J. Geophys. Res.* **73,** 6085–97.
Gast, P. W. (1968) *Geochim. Cosmochim Acta*, **32,** 1057–85.
Gordon, G. E., Randle, K., Goles, G. G., Corliss, J. B., Beeson, M. H., and Oxley, S. S. (1968) Ibid. **32,** 369–96.
Hanson, G. N. (1978) *Earth Planet. Sci. Lett.* **38,** 26–43.
Herrmann, A. G. (1970) Yttrium and Lanthanides. In *Handbook of Geochemistry II/5.* Springer-Verlag, Berlin.
Hertogen, J., and Gijbels, R. (1971) *Anal. Chim. Acta*, **56,** 61–82.
Jacobs, J. W., Korotev, R. L., Blanchard, D. P., and Haskin, L. A. (1977) *J. Radioanal. Chem.* **40,** 93–114.
Kay, R. W., and Hubbard, N. J. (1978) *Earth Planet. Sci. Lett.* **38,** 95–116.
Khan, I. H. (1972) *Geochemistry of the aureole of the Land's End granite.* Ph.D. thesis, University of Birmingham (unpubl.).
Leake, B. H., Hendry, G. L., Kemp, A., Plant, A. G., Harvey, P. K., Wilson, J. R., Coats, J. S., Aucott, J. W., Lunel, T., and Howarth, R. J. (1969) *Chem. Geol.* **5,** 7–86.
Mitropoulos, P. (1979) *A contribution to the REE and trace element geochemistry of the Land's End granite aureole, SW England.* Ph.D. thesis, University of Birmingham (unpubl.).
——(1982) *Chem. Geol.* **35,** 265–80.
Plant, J., Goode, G. C., and Herrington, J. (1976) *J. Geochem. Explor.* **6,** 299–319.
Sun, S. S., and Hanson, G. N. (1975) *Contrib. Mineral. Petrol.* **52,** 77–106.
Wood, D. A., Gibson, I. L., and Thompson, R. N. (1976) Ibid. **55,** 241–54.

[*Manuscript received 27 January 1984; revised 18 April 1984*]